ChemPubSoc Europe

DOI: 10.1002/chem.201502434

CHEMISTRY A European Journal Full Paper

Self-Assembly

Spacer-Modulated Differentiation Between Self-Assembly and Folding Pathways for Bichromophoric Merocyanine Dyes

André Zitzler-Kunkel, Eva Kirchner, David Bialas, Christian Simon, and Frank Würthner*[a]

Abstract: We have synthesized a large series of bis(merocyanine) dyes with varying spacer unit and investigated in detail their self-organization behavior by concentration- as well as solvent-dependent UV/Vis spectroscopy. Our in-depth studies have shown that the self-organization of the present bis(merocyanine) dyes is subtly influenced by the nature of the spacer unit. The utilization of rigid spacers results in the formation of self-associated bimolecular complexes with high binding strength, while flexible spacers drive the respective bichromophoric dyes to intramolecular folding. Our thorough investigations on the impact of alkyl spacer chain length on the folding tendency of the present series of bis(merocyanine) dyes revealed a biphasic behavior, that is, a steep increase of the folding tendency for the dyes containing C4 to C7 chains and then a gentle decrease for dyes with longer alkyl spacer chains as evidenced by free energy (ΔG) values for the folding of these dyes. Furthermore, analyses of aggregates' optical properties based on exciton theory as well as quantum chemical calculations suggest a bimolecular aggregate structure for the dye possessing a rigid spacer and a rotationally twisted pleated structure for the bis(merocyanine) dyes having spacer units with less than seven carbon atoms, while the application of longer alkyl chain linkers ($\geq$C7) provides enough flexibility to orient the chromophores in electrostatically most favored antiparallel fashion.

Introduction

Appreciable changes of intrinsic optical[1] and electronic[2] properties of molecular dyes upon aggregation offer unique opportunities both for the advancement of supramolecular chemistry and development of organic materials for electronics, photonics, or photovoltaics.[3] Accordingly, significant efforts have been devoted to control the packing of molecular dyes in self-assembled materials[4] and a plethora of topologies (stacks, cycles, polyhedra, micelles, vesicles, layers, liquid crystals, etc.) have meanwhile been realized. In contrast to this tremendous effort on *inter*molecular self-assembly, far less examples are known where dye aggregation is directed by *intra*molecular folding.[5] This is particularly surprising if we consider the increasingly growing interest in foldamers,[6] and the fact that the proper folding of biomacromolecules in natural systems into a particular conformation is prerequisite for the realization of highly ordered architectures with pivotal functions as evidenced by, for example, multi-protein complexes of the ribosome, virus capsids and the photosystems in plants and bacteria.[7] Indeed, within the research field of peptide-based supramolecular π-conjugated materials,[8] the relevance of folding has been well recognized and utilized toward tailored structures and functions by folding-driven self-assembly.[9] While this research takes advantage of meanwhile well-established peptide sequences that direct particular folding patterns such as α-helices, β-turns,[10] no such structure-folding property relationships are available for the design of backbone-directed aromatic π-stacks. Although the design of tweezers for the complexation of aromatic molecules has been approached in great detail[11] and some examples of folding-driven dye aggregation are known,[5] apparently studies devoted to the here addressed question of "folding versus self-assembly", that is, backbone-driven differentiation between *intra*molecular folding and *inter*molecular self-assembly pathways (see the illustration in Scheme 1, bottom), have only been scarcely attended for π-conjugated dye molecules.[12] In particular, studies related to the impact of the chain length and constitution of a linking tether between two dye molecules are obviously missing.

Our recent research activities on merocyanine dye aggregates suggest that these dyes are particularly suited for such investigations due to their following outstanding features: i) This class of dyes show very distinct spectral changes in the UV-visible spectral range upon aggregation (enabling easy monitoring),[13] and ii) the binding strength between merocyanines is quite high due to pronounced electrostatic support (dipole–dipole interaction) to the attractive forces evoked by dispersion forces between aromatic scaffolds that ensure aggregation either by folding or self-assembly.[14] Moreover, in a recent communication we could demonstrate that an optimized processing procedure taking advantage of a folding-driven self-assembly sequence of bis(merocyanine) dye **1 d** (see

[a] *Dr. A. Zitzler-Kunkel, E. Kirchner, D. Bialas, C. Simon, Prof. Dr. F. Würthner*
Universität Würzburg
Institut für Organische Chemie & Center for Nanosystems Chemistry
Am Hubland, 97074 Würzburg (Germany)
Fax: (+49) 931-31-84756
E-mail: wuerthner@chemie.uni-wuerzburg.de

Supporting information for this article is available on the WWW under http://dx.doi.org/10.1002/chem.201502434.

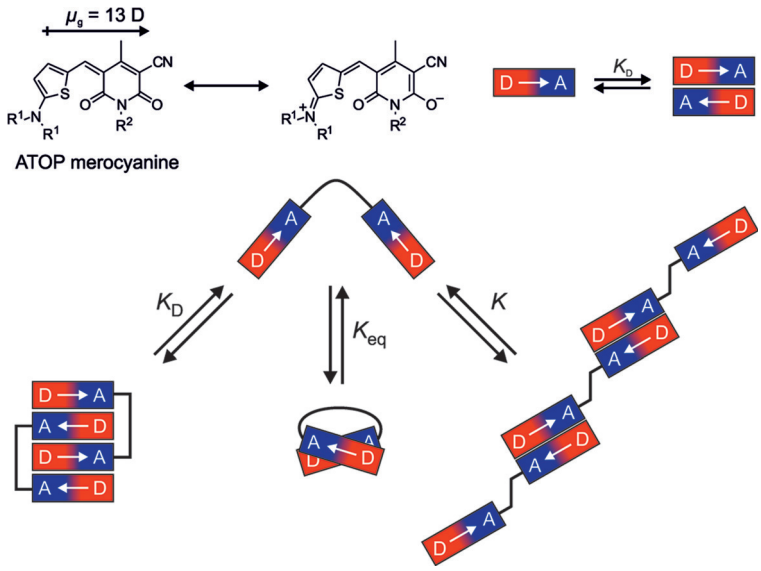

Scheme 1. Resonance structures and schematic illustration of the dimerization of mono-(ATOP) merocyanine dyes (top) by dipolar interactions and different pathways for the spacer-modulated self-organization of bichromophoric ATOP merocyanine dyes (bottom) into well-defined bimolecular complexes (left), extended supramolecular polymers (right), or the formation of intramolecularly folded structures (middle).

Scheme 3) afforded bulk heterojunction solar cells with improved photocurrents, pinpointing the impact of supramolecular order on the functional properties of a material.[15] These promising preconditions motivated us towards a fundamental study devoted to self-organization behavior of molecular architectures in which two merocyanine dyes are tethered by spacer units of different length and stiffness. Accordingly, we have synthesized a broad series of bis(merocyanine) dyes and studied their aggregation behavior in comparison to the parent *a*mino-*t*hienyl-di*o*xocyano-*p*yridine (ATOP) chromophore (Scheme 1, top), which was introduced more than a decade ago as a superb merocyanine dye for photorefractive materials due to its narrow cyanine-type absorption features ("merocyanine in the cyanine limit") and large dipole moment of 13 D entailed by its pronounced zwitterionic character.[16]

Here we report that, to our surprise, all of the presently investigated bis(merocyanine) dyes with (sufficiently long) flexible tethers preferred the *intra*molecular folding pathway (Scheme 1, middle), except one dye bearing a more rigid tether that self-assembled *inter*molecularly into a bimolecular complex (Scheme 1, left). The third option (Scheme 1, right), that is, the formation of supramolecular polymers,[17] was not observed for the present series of bis(merocyanine) dyes within the concentration range of our study.

Results

Synthesis

The synthetic route to the merocyanine dyes **1a–k** is outlined in Scheme 2 and their full chemical structures are shown in Scheme 3. In the first synthetic step, amidisation of cyanoacetic acid methyl ester ($NCCH_2CO_2Me$) with the primary amines **2a–k**, which are either commercially available or prepared according to literature, under solvent-free conditions at ambient temperature afforded the corresponding amides **3a–k** in high yields. Subsequently, the condensation reaction of cyanoacetic acid amides **3a–k** with ethyl acetoacetate resulted in the corresponding hydroxypyridones **4a–k** that were typically used as obtained (purity >90%) for further reaction. In the final step, a Knoevenagel condensation reaction of 5-dibutylamino-thiophene-2-carbaldehyde with these hydroxypyridones **4a–k** in acetic anhydride afforded the desired merocyanine dyes **1a–k** in 41–93% yields. All unknown target compounds **1c,e–k** were characterized by ^1H and ^{13}C NMR, high resolution mass spectrometry, UV/Vis spectroscopy, and elemental analysis (for details see the Experimental Section).

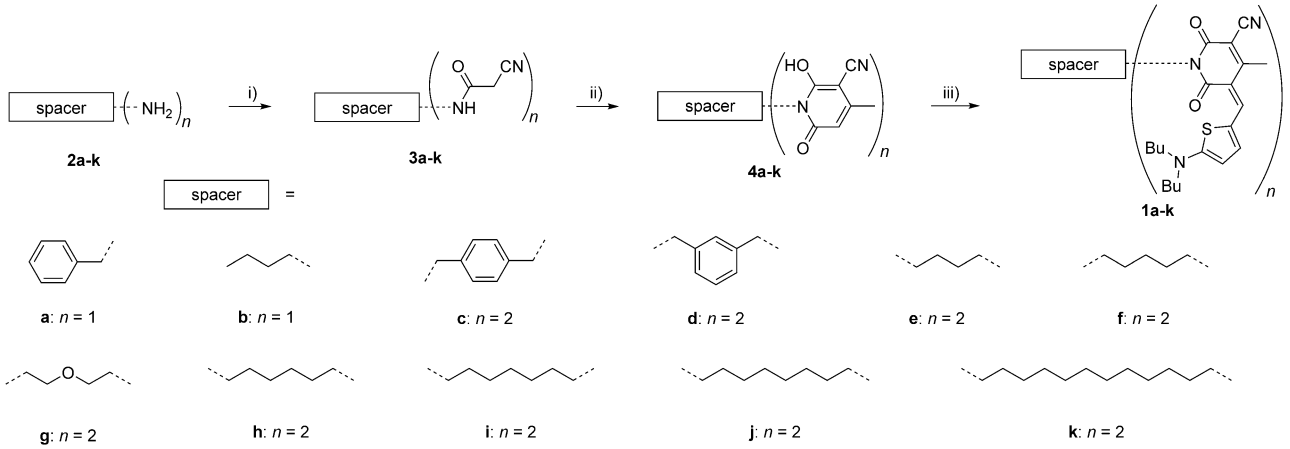

Scheme 2. Synthesis of merocyanine dyes **1a–k**. i) $NCCH_2CO_2Me$, 25 °C, 4 h, yields 81–97%; ii) $AcCH_2CO_2Et$, piperidine, 100 °C, 4–24 h, yields 74–94%; iii) 5-dibutylaminothiophene-2-carbaldehyde, Ac_2O, 90 °C, 1 h, yields 41–93%.

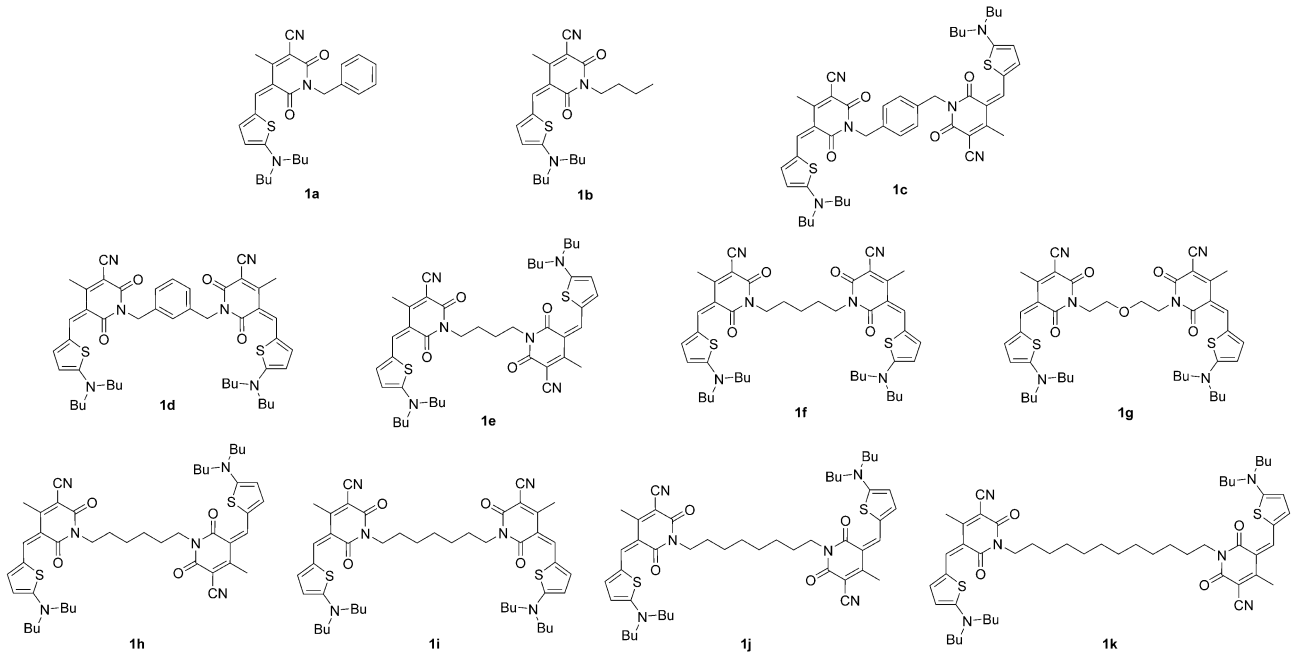

Scheme 3. Chemical structures of the merocyanine dyes **1a**–**k** investigated in this work.

Concentration-Dependent UV/Vis Studies

The self-organization behavior of mono(merocyanine) reference dyes **1a**,**b** and bis(merocyanine) dyes **1c**–**k** that bear different spacer units was first explored by concentration-dependent UV/Vis experiments in nonpolar dioxane, since this solvent has turned out to be ideal for the study of self-organization of the present series of dyes in the concentration regime appropriate for UV/Vis spectroscopy. By employing concentration-dependent UV/Vis spectroscopy, the aggregation mechanism for different dye molecules can be elucidated by fitting the absorption data to appropriate mathematical models.[14] Moreover, initial structural information can be derived from the spectral position and splitting of the aggregate absorption band by comparison with that of the monomer band, which would then allow a classification to H- or J-type[1] excitonic coupling[18,19] between the interacting transition dipole moments of adjacent chromophores. The precise magnitude of the spectral shift is thereby strongly dependent on the translational and rotational offset between the two interacting chromophores.[18,19] The UV/Vis spectra of the present merocyanine dyes were measured in dioxane in the concentration range of around 10^{-8} to 10^{-3} M (depending on the solubility properties of the dyes). As representative examples, the concentration-dependent spectra of reference mono(merocyanine) dye **1a** and those of bis(merocyanine) dyes **1c**, **1i** and **1k** with *p*-xylylene, heptyl and dodecyl spacer, respectively, are depicted in Figure 1. The spectra of the remaining merocyanines are shown in Supporting Information (Figure S1). As shown in Figure 1a,b, for the reference dye **1a** and bis(merocyanine) **1c**, the variation of concentration resulted in significant spectral changes. Thus, with decreasing concentration a gradual decrease of the H-type aggregate band (denoted as H) with absorption maximum at 505 nm for **1a** and 479 nm for **1c**, and a concomitant appearance of a bathochromically shifted intense charge transfer band centered at around 536 nm (denoted as M), which corresponds to the respective monomeric species,[16] were observed. The calculated aggregate spectra of **1a** and **1c** also visualize next to the intense H-band a second transition at longer wavelength (J-band), which is suggestive of a slightly twisted arrangement of the interacting transition dipole moments that are oriented along the long molecular axis of the chromophores.[20] Over the whole investigated concentration range very clear isosbestic points were observed in the spectra of both dyes **1a** and **1c** which indicate a thermody-

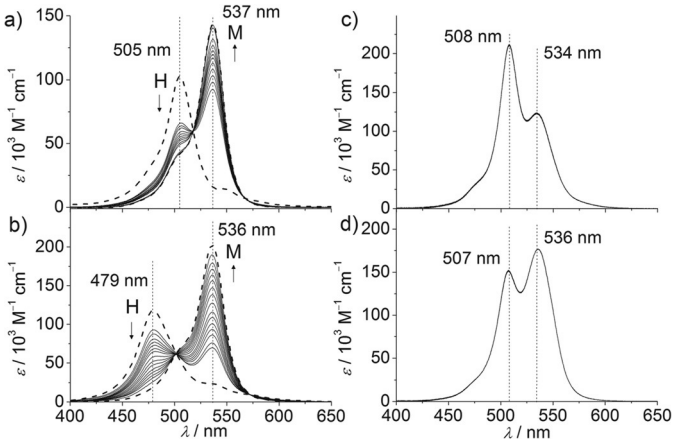

Figure 1. Concentration-dependent UV/Vis spectra of a) **1a** ($c = 3\times10^{-5}$–4×10^{-3} M), b) **1c** ($c = 9\times10^{-8}$–1×10^{-5} M), c) **1i** ($c = 3\times10^{-7}$–1×10^{-5} M) and d) **1k** ($c = 5\times10^{-7}$–1×10^{-5} M) in dioxane at 298 K. Arrows indicate the spectral changes upon dilution. The dotted lines in a) and b) correspond to the calculated ideal monomer and dimer spectra, respectively.

namic equilibrium between the respective monomeric and the aggregated species. Similar spectroscopic changes were observed for the monomeric reference **1b** (see Supporting Information, Figure S1a).

In striking contrast to the spectra of references **1a**,**b** and those of bis(merocyanine) **1c**, the absorption spectra of the remaining bis(merocyanine) dyes **1d**–**k** do not show appreciable changes upon dilution, even not at a very low concentration of only about $c \approx 1 \times 10^{-7}$ M (see Figure 1c,d and Figure S1b–h). However, over the whole concentration range, for these bis(merocyanine) dyes (**1d**–**k**) a hypsochromically shifted band (H-band) of an exciton-coupled merocyanine dimer aggregate[21] was observed, respectively, in coexistence with the band at around 535 nm for uncoupled chromophores. Thus, this H-band has to be attributed to the presence of intramolecular folded structures, in which the excitonic coupling occurs due to the close proximity of two π-stacked merocyanine dyes.

Solvent-Dependent UV/Vis Studies

We have previously shown that, due to the accessibility of broad solvent permittivity range, tetrahydrofuran (THF; $\varepsilon_r = 7.58$)/methylcyclohexane (MCH; $\varepsilon_r = 2.02$) solvent mixtures are highly suitable to study merocyanine dye aggregation.[15,22] In nonpolar MCH aggregation of dipolar merocyanines is favored, while the interaction of dipole moments of dyes with polar THF stabilizes the monomeric species with respect to the aggregate.[23] Thus, to get more insight into the self-organization processes of the bis(merocyanine) dyes **1d**–**k**, which do not display any considerable changes in their absorption spectra upon dilution in dioxane, we have performed solvent-dependent UV/Vis measurements in THF/MCH mixtures by increasing the volume fraction of nonpolar MCH from 0 up to 90% under dilute ($c = 1 \times 10^{-6}$ M) conditions. For comparison, solvent-dependent spectra of reference dye **1a** were measured under the same conditions. Solvent-dependent spectra of bis(merocyanines) **1e**, **1i** and **1k** are shown as examples in Figure 2 and those of reference **1a** and remaining bis(merocyanine) dyes (**1d**,**f**,**g**,**h**,**j**) are displayed in Supporting Information (Figure S2). While the solvent-dependent spectral changes for the mono(merocyanine) **1a** are rather negligible, substantial changes were observed for the bis(merocyanine) dyes **1d**–**k**. Among the alkyl chain (C4-C8 and C12) spacer bearing bis(merocyanine) dyes, for dye **1e** (C4 spacer) less pronounced spectral changes were observed with a moderate decrease of the monomer band at 536 nm and emergence of a weak blue-shifted shoulder at 518 nm upon increasing the volume fraction of MCH (Figure 2a). These observations suggest that the C4 spacer is too short to effect the stacking of the two merocyanine dyes on top of each other in a common antiparallel arrangement. For other alkyl-spaced bis(merocyanine) dyes considerably stronger spectral changes were observed with varying solvent composition. For example, in the case of **1i** with C7 spacer the monomer band at 536 nm was vanished with a concomitant appearance of a hypsochromically shifted intense band centered at 505 nm upon increasing the content of MCH up to 90% (Figure 2b). Nearly identical observation was made for **1j** with C8 spacer (Figure S2f). A similar trend was also observed for the dye **1k** bearing C12 spacer, but the monomer band at 536 nm was still evident at a THF/MCH ratio of 10:90 (Figure 2c) which might indicate a weaker aggregation propensity of this dye compared to that of **1j** (C8 spacer). The solvent-dependent spectral changes of **1f** (C5 spacer), **1g** (3-oxopentyl spacer) and **1h** (C6 spacer) resemble those of C12-tethered dye **1k** (see Figure S2c,d,e and Figure 2c). The solvent-dependent spectral changes of bis(merocyanine) dyes **1e**–**k** are accompanied by a clear quasi-isosbestic point, respectively, as observed previously for dye **1d** with *m*-xylylene spacer,[15] revealing a chemical equilibrium between two species, that is, the folded and the unfolded conformers of these molecules.

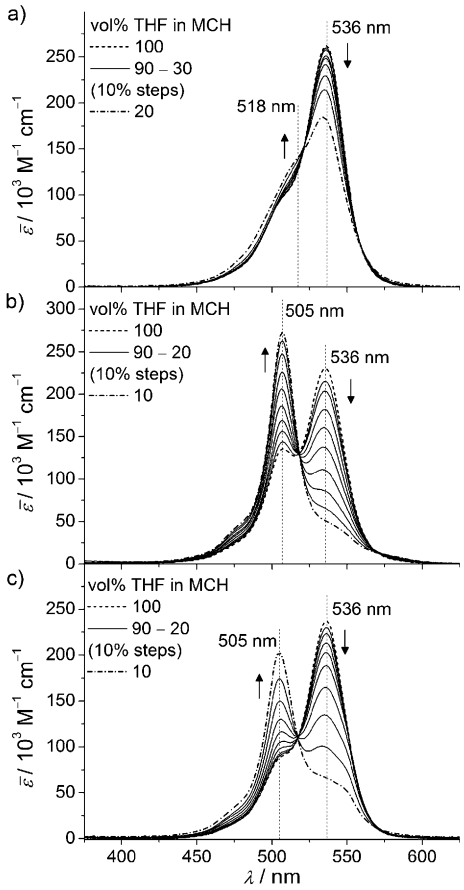

Figure 2. Solvent-dependent UV/Vis spectra of the bis(merocyanine) dyes a) **1e**, b) **1i** and c) **1k** in THF/MCH mixtures ($c = 1 \times 10^{-6}$ M, $T = 298$ K) starting in pure THF (dotted lines) and successively increasing the volume fraction of MCH up to 90% (dashed-dotted lines). Arrows indicate the spectral changes upon increasing the volume fraction of MCH.

DFT Calculations

To rationalize our spectroscopic observations, DFT calculations (B97D3/def2-SVP) were performed for the monomers of bis(merocyanine) dyes **1i**, **1d** and **1c** as well as for the bimolecular complex of **1c** (Figure 3, for further information see Supporting Information). While the chromophores of **1i** with flexible C7 alkyl spacer are planar and exhibit an ideal distance of

3.4 Å for π-stacking (Figure 3a), one observes a larger distance in **1d** (*m*-xylylene spacer) of 3.8 Å and a bending of the chromophores, indicating a comparatively less favorable folded state due to the rigid spacer unit (Figure 3b). The geometry-optimized structure of monomer **1c** shows an even larger distance of 4.0 Å and a strong bending of the chromophores since the *p*-xylylene spacer unit does not allow a perfect alignment of the chromophores for geometric reasons and thus disfavors the folded state (Figure 3c). Instead, the dimer structure shown in Figure 3d, which represents a stack of four merocyanine chromophores with smaller distances of 3.3 and 3.4 Å, should be more favored. This bimolecular aggregate structure is feasible since the *p*-xylylene spacer allows intercalation of an additional chromophore between two merocyanine units of a molecule with a perfect π-stacking distance of ~3.4 Å.[24] By comparing the DFT energies of the monomer and the dimer of **1c**, it becomes apparent that the energy gain for the formation of the dimer amounts to 0.0530 a.u. (139 kJ mol^{-1}) per molecule which can be attributed to the close packing of the chromophores in the quadruple merocyanine stack. For comparison, the intermolecular distances that were found in single crystals of reference merocyanine **1a** are 3.5 and 3.6 Å,[25] which are even slightly larger than the distances calculated for the dimer structure of **1c**.

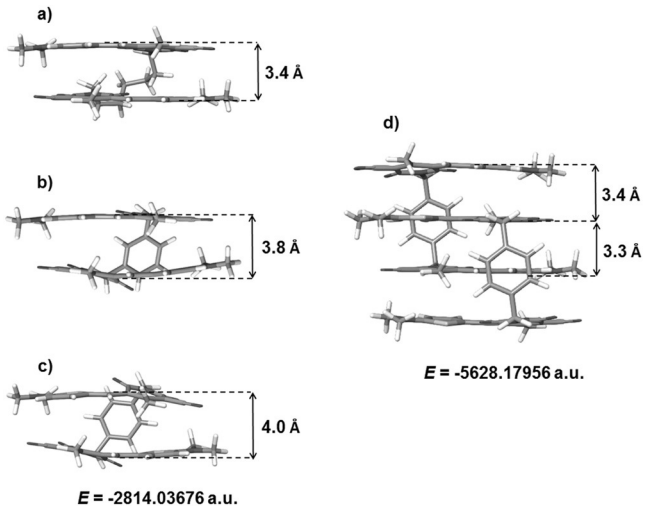

Figure 3. Geometry-optimized structures in side view of monomers a) **1i**, b) **1d** and c) **1c** as well as d) the dimer of **1c** obtained by DFT calculations (B97D3/def2-SVP, butyl groups were replaced by methyl groups).

Discussion

Evaluation of Self-Assembly Mechanism For Bis(merocyanine) Dye 1c Based on Concentration-Dependent UV/Vis Spectral Data

The existence of clear isosbestic points in the concentration-dependent UV/Vis spectra (in dioxane) of the reference mono(merocyanines) **1a**,**b** and bis(merocyanine) dye **1c** substantiates a chemical equilibrium between monomeric and aggregated species and allows a thermodynamic analysis of the self-assembly process. For a quantitative description of the aggregation process, initially the simplest mathematical models, these are the dimerization[13,14] and the isodesmic or equal *K* model,[14,26,27] were applied to fit the experimentally obtained data points. As expected based on our previous work on the aggregation of simple ATOP merocyanine dyes,[13] for the reference dyes **1a**,**b** the spectral changes could appropriately be described with the dimerization model (Figure 4), while the isodesmic model was not applicable to describe their aggregation process. On the other hand, it is surprising that the concentration-dependent spectral changes observed for bis(merocyanine) dye **1c** could also be nicely fitted with the dimerization model, although our previous work on another class of bis(merocyanine) dyes bearing *p*-xylylene spacer unit afforded supramolecular polymers[28] as depicted in Scheme 1 (on the right). This illustrates that subtle changes in conformational preferences and sterical demands have a strong impact on the formation of preferred self-assembly product.

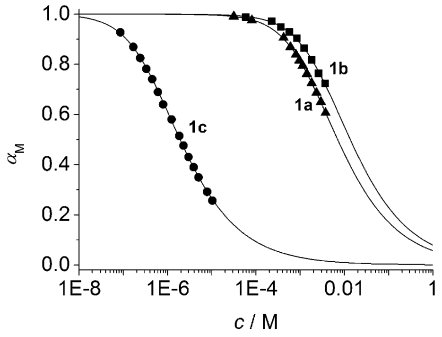

Figure 4. The fraction of monomeric species α_M calculated from the UV/Vis data at a certain wavelength and results of the nonlinear regression analysis based on the dimerization model for dyes **1a** (▲; 537 nm), **1b** (■; 537 nm) and **1c** (●; 536 nm) in dioxane.

For the analysis, a monomer-dimer equilibrium of dyes is assumed in solution for which the dimerization constant K_D is defined by the law of mass action according to Equation (1).

$$K_D = \frac{c_D}{c_M^2} = \frac{1-\alpha_M}{2\alpha_M^2 c_0} \quad (1)$$

Herein c_M and c_D are the concentrations of the monomeric and dimeric species, respectively, c_0 is the total dye concentration and α_M is the fraction of monomeric species in solution.[13] By solving this equation and taking into account the average absorptivity ($\bar{\varepsilon}$) of a dye in solution, which is the sum of the contributions of monomeric and dimeric species as shown in Equation (2):

$$\bar{\varepsilon} = \varepsilon_M \alpha_M + (1-\alpha_M)\varepsilon_D \quad (2)$$

where ε_M and ε_D denote the normalized molar absorptivities of the monomer and dimer, respectively, we obtain Equation (3):

$$\bar{\varepsilon} = \frac{-1 + \sqrt{8K_D c_0 + 1}}{4K_D c_0} (\varepsilon_M - \varepsilon_D) + \varepsilon_D \quad (3)$$

Nonlinear regression analysis of the experimentally determined extinction coefficients as a function of total dye concentration c_0 at certain wavelengths affords the dimerization constants K_D and enables the calculation of the associated Gibbs free dimerization energies (ΔG_D^0) according to the Equation (4):

$$\Delta G_D^0 = -RT \ln K_D \quad (4)$$

As it is evident from the results summarized in Figure 4 and Table 1, bis(merocyanine) dye **1c** displays significantly higher (three orders of magnitude) dimerization constant ($K_D = 5.4 \times 10^5$ M^{-1}) compared to those of the reference dyes **1a** and **1b** ($K_D = 1.7 \times 10^2$ and 1.2×10^2 M^{-1}). Such a strong increase in the binding strength for **1c** may be rationalized by the presence of three electrostatically (dipole–dipole interactions) and also with regard to dispersion interactions favorable contacts between closely stacked dyes in a bimolecular π-stack composed of four chromophoric units (see Figure 3d). Accordingly, the dimerization takes place already at concentrations around 10^{-5} M, whereas the competing pathway towards supramolecular polymers would only initiate at concentrations of around 0.01 M (where the monomeric dyes **1a**,**b** self-assemble into dimeric units). However, above a certain concentration, that is, the effective molarity (*EM*),[29] a transition from cyclic aggregates (i.e., the dimer of **1c**) into supramolecular polymers might occur. As this concentration is >1 M (estimated from $EM = K_D(\mathbf{1c})/[4 \times K_D(\mathbf{1a})]^2$), which is far above the concentration regime of our concentration-dependent UV/Vis measurements, the formation of linear oligomers by supramolecular polymerization can be excluded for bis(merocyanine) **1c**.

Table 1. Dimerization constants K_D in dioxane for dyes **1a-c** and corresponding standard Gibbs free dimerization energies ΔG_D^0 from analysis based on the dimerization model and absorption maxima of reference dyes **1a**,**b** and bis(merocyanine) dye **1c**.

Dye	K_D[a] [M^{-1}]	ΔG_D^0 [kJ mol^{-1}]	λ_M [nm]	λ_{agg1} [nm]	λ_{agg2} [nm]	$\Delta\bar{\nu}_{agg1-M}$ [cm^{-1}]
1a	1.7×10^2	−12.4	537	505	547	1180
1b	1.2×10^2	−11.9	537	506	549	1141
1c	5.4×10^5	−32.7	536	479	–	2220

[a] Averaged from multilinear regression analysis around the absorption maximum of the monomer ($\lambda_M \pm 10$ nm) or dimer band ($\lambda_D \pm 10$ nm), respectively.

A comparison of the aggregate band's spectral position for reference dye **1a** (505 nm) or **1b** (506 nm) with that of bis(merocyanine) **1c** (479 nm) shows that the latter is much more blue shifted with respect to the monomer band (~536 nm). This observation corroborates the suggestion that a bimolecular π-stack is formed from **1c** because the interaction of an increasing number of transition dipole moments in an aggregate stack should result in a more pronounced spectral shift of the aggregate absorption band $\Delta\bar{\nu}_{D\text{-}M}$ in accordance with exciton theory (Figure 5).[18,19] Unfortunately, due to its forbidden nature, the position of the lowest energy excitonic state cannot be assigned from our concentration-dependent UV/Vis spectra (Figure 1) for the tetramer stack of **1c** (i.e., bimolecular assembly of two **1c** molecules). Hence, the excitonic coupling ε can only be estimated from $\varepsilon \approx \Delta\bar{\nu}_{agg1-M}$ which is indeed almost doubled for the tetrameric stack compared to that of the dimeric stack of **1a** or **1b** (see Table 1).

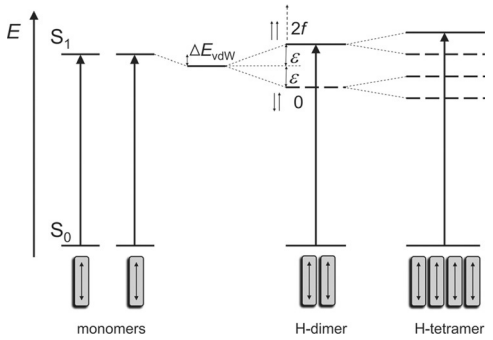

Figure 5. Schematic energy level diagram illustrating allowed electronic transitions (long arrows) for monomers, H-dimers and H-tetramers according to the molecular exciton theory. The dipole phase relations for the H-dimer are also shown. ε is the excitonic coupling and *f* the oscillator strength of the optical transition, which is for perfectly coplanar transition dipole moments doubled for the H-band and zero for the J-band according to Kasha theory.[18,19]

Evaluation of Folding Mechanism for Bis(merocyanine) Dyes 1d–k Based on Solvent-Dependent UV/Vis Data

The concentration-dependent UV/Vis spectra of bis(merocyanine) dyes **1d–k** in dioxane display a linear increase of absorption with increasing concentration in accordance with Lambert–Beer's law for the entire investigated concentration range. Thus, no changes are observed for the absorption coefficient ε for the whole wavelength range over more than a 100-fold variation in concentration. Although these results rule out the presence of self-assembly processes, the shape of the absorption bands indicates different degrees of folding. Thus, some dyes such as **1i** exhibit the most intense band at 508 nm, which is close to the position of the hypsochromically shifted dimer aggregate band of reference dyes **1a**,**b**, whilst other dyes such as **1k** show the strongest absorption at the position of the monomer band at 536 nm and only smaller absorption for the hypsochromically shifted band. Thus, these bands can be attributed to the presence of two different conformational states, that is, folded and unfolded conformations, whereby the former consists of antiparallel stacked dyes and the latter prevails without close dye-dye contacts and hence exhibits negligible excitonic coupling.

The equilibrium between unfolded and folded species for dyes **1d–k** could be monitored by solvent-dependent UV/Vis studies in THF/MCH mixtures (Figure 2 and Figure S2). In the conducted experiments a clear quasi-isosbestic point, respectively, was observed for all of these bis(merocyanine) dyes, cor-

roborating the two-state equilibrium according to Equation (5). For such situations the thermodynamic driving force for the folding process may be analyzed according to a model established by Moore and Ray[30] to determine the equilibrium constants K_{eq} and the free energy changes ΔG.

$$\text{unfolded state} \overset{K_{eq},\ \Delta G}{\rightleftharpoons} \text{folded state} \tag{5}$$

For the determination of thermodynamic data, the solvent-dependent absorption coefficients at the center of the aggregate band (λ_{agg} in Table 2) are most useful, although other wavelengths might be utilized as well. Towards a straightforward procedure, initially two assumptions have to be made. First, we assume that the extinction values ε_U obtained in pure THF correspond to the state where the bis(merocyanine) dyes are entirely unfolded. Second, as the dyes are not soluble in pure MCH, we assume that at least for dyes **1d**,**i**,**j** with the strongest folding tendency in the most nonpolar solvent mixture (THF/MCH = 10:90) the extinction values ε_F coincide with the state where these bis(merocyanine) dyes are completely folded.

Table 2. Extrapolated Gibbs free energy changes in MCH derived from the analysis of folding process in THF/MCH mixtures, slope of the fitting line *m* and absorption maxima and wavelength shifts of folded bis(merocyanine) dyes **1d**–**k** in MCH compared to monomeric dyes.

Dye	ΔG(MCH) [kJ mol^{-1}]	m [kJ mol^{-1}]	λ_M [nm]	λ_{agg} [nm]	$\Delta\tilde{\nu}_{agg\text{-}M}$ [cm^{-1}]
1d	−7.3 ± 0.5	158 ± 9	536	513	836
1e	1.9 ± 0.4	123 ± 8	536	516	723
1f	−2.6 ± 0.3	135 ± 5	535	513	802
1g	−5.2 ± 0.2	141 ± 4	535	514	764
1h	−2.9 ± 0.2	136 ± 4	536	510	951
1i	−8.9 ± 0.5	169 ± 9	536	505	1145
1j	−7.6 ± 0.4	163 ± 8	536	505	1145
1k	−3.9 ± 0.2	153 ± 4	536	505	1145

However, for the dyes **1e**–**h**,**k** with a distinctly lower folding tendency this assumption obviously does not hold true. Therefore, we make the simplified but reasonable approximation that fully folded molecules would show extinction value ε_F for their foldamer H-band that are equal to the extinction value ε_U of the unfolded species of the respective dye in pure THF (at the monomer M-band). Based on these considerations, the mole fraction of the dyes in the unfolded state $\alpha_{unfolded}$ can be calculated for all solvent compositions using Equation (6).

$$\alpha_{unfolded} = \frac{\varepsilon(\lambda)_F - \varepsilon(\lambda)}{\varepsilon(\lambda)_F - \varepsilon(\lambda)_U} \tag{6}$$

Herein $\varepsilon(\lambda)$ denotes the extinction value at a particular wavelength (λ) for an intermediate solvent composition and $\varepsilon(\lambda)_F$ and $\varepsilon(\lambda)_U$ are the respective values for fully folded and fully unfolded species that are different at this wavelength. The equilibrium constant K_{eq} and related Gibbs free energy changes ΔG for the conformational transition for any solvent composition can then be obtained from the following relationships:

$$K_{eq} = \frac{c_F}{c_U} = \frac{1 - \alpha_{unfolded}}{\alpha_{unfolded}} \tag{7}$$

$$\Delta G = -RT \ln K_{eq} \tag{8}$$

where c_F and c_U represent the concentration of the folded and unfolded species, respectively. The free energy change between both conformational states is assumed to linearly depend on solvent composition in analogy to the solvent denaturation of proteins and peptide secondary structures.[31] This enables an extrapolation of the free energy change in pure MCH (ΔG(MCH)) by linear regression analysis of the free energy values obtained for intermediate solvent compositions according to Equation (9).

$$\Delta G = \Delta G(\text{MCH}) - m[\text{THF}] \tag{9}$$

Based on this analytical procedure, we obtain the data depicted in Figure 6 and the corresponding numerical values are compiled in Table 2. Detailed thermodynamic data obtained by this analysis are shown in Supporting Information (Table S1). In Figure 6a it can be clearly seen that the free energy changes for the transition region between 20–80 vol% THF follow the assumed linear dependency on the solvent composition. If we plot the obtained free energy changes ΔG(MCH) for pure MCH against the number of atoms in the tether unit, we obtain the relationship shown in Figure 6b. There are two interesting features to discuss in this plot: The first one is the dependence of folding on the number of carbon atoms present in the aliphatic tether units (connected by dashed line) and the second one is the varying spacer units with a chain length of five atoms that are different in element and/or their conformational degree of freedom. Regarding the bis(merocyanine) dyes with different lengths of the alkyl linkers, two regimes can be clearly distinguished. For C4 to C7 chains a strong linear increase in the folding tendency is observed. On the other hand, if the chain length is further increased, a comparatively less intense decrease of the folding tendency is observed with increasing chain length. Based on our results discussed above, we can conclude that within the range of C5 to C12 alkyl chain lengths, the respective folded species is thermodynamically more stable in pure MCH. For the shorter linker C4, the energetic benefit from dye-dye interactions is obviously not sufficient to overcome the required distortion of the linker units and hence this molecule prevails in the open state even in the least polar solvent MCH. Accordingly, C4 or shorter linkers would be the choice if supramolecular polymers, as shown in Scheme 1 (on the right), are targeted. A limited solubility of these dyes in MCH prohibits such studies as higher concentrations would be required.

If we now analyze the folding tendencies of the dyes **1d**,**f**,**g** bearing different spacers that comprise five linking atoms, we notice a strong dependence on the nature of the spacer unit. The free energy change in pure MCH markedly increases from pentyl (**1f**; ΔG(MCH) = −2.6 ± 0.3 kJ mol^{-1}) via 3-oxapentyl (**1g**; ΔG(MCH) = −5.2 ± 0.2 kJ mol^{-1}) to the *m*-xylylene (**1d**; ΔG(MCH) = −7.3 ± 0.5 kJ mol^{-1}) spacer unit. The crucial part of

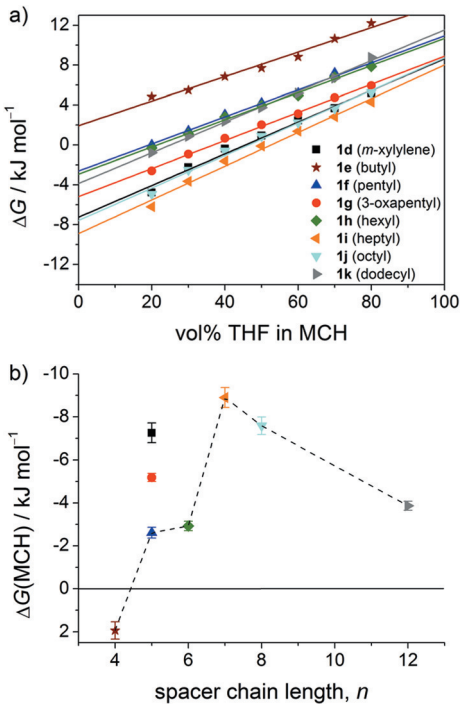

Figure 6. a) Plot of the ΔG values for the folding process of bis(merocyanine) dyes **1 d**–**k** derived from the spectral development at the respective maximum of the H-aggregate band. The solid lines represent the respective fitting curves from linear regression analysis according to Equation (9). b) Plot of the free energy change ΔG(MCH) as the y-intercept from the analysis in a) as a function of the alkyl chain length of the spacer unit.

the spacer units involves the six bonds between the imide N atoms at which the two merocyanine chromophore units are tethered. As only four of these six bonds are freely rotatable for the *m*-xylylene spacer (**1 d**), we attribute its highest folding tendency among these three dyes **1 d**,**f**,**g** to a better preorganization of the linker with regard to the π-stacked folded structure. Accordingly, for dye **1 d** only four rotational degrees of freedom have to be frozen out in the folded conformer in contrast to six for dyes **1 f**,**g**, respectively. For this reason the folding of **1 d** should be entropically favored.[32] For **1 f**,**g**, however, the number of rotable bonds is equal. Here, the 3-oxapentyl chain in **1 g** obviously exhibits a higher flexibility of the linker compared to that of the pentyl chain which prefers a linearly stretched-out conformation (all-*trans*).[33] Therefore, the oxygen atom in the spacer unit facilitates the folding.

Structural Insights in Foldamers Based on Exciton Theory

Our previous work on self-assembled dimers of dipolar merocyanine dyes such as reference compounds **1 a**,**b** and related merocyanines with various donor and acceptor heterocycles suggested sandwich-type co-facially stacked centrosymmetric dimer aggregate structures.[13,25] Because the transition dipole moments (relevant for exciton coupling) are not perfectly collinear with the dipole moments (which direct the antiparallel arrangement) and, in addition to the dipole–dipole interaction, dispersion forces have also an influence on the particular aggregate structure, we cannot assume a perfect H-coupling situation. This is corroborated by a non-negligible absorption for the lower energy J-transition for self-assembled merocyanine dimer aggregates (see Figure 1 a). Indeed, the intensity of this band might be utilized to calculate the rotational offset from the perfect antiparallel arrangement.[19,20] Because this intensity is, however, prone to significant errors due to the required extrapolation from concentration-dependent studies, we will here perform an analysis based on the experimentally better defined exciton coupling energy $\varepsilon \approx \Delta\tilde{\nu}_{\text{agg-M}}$ values (Table 2) according to Equation (10).

$$\varepsilon = \frac{|\vec{\mu}_{\text{ag}}|^2}{4\pi\varepsilon_0 r_{\text{AB}}^3}(\cos\alpha - 3\cos^2\theta) \qquad (10)$$

Herein, μ_{ag} denotes the transition dipole moment of the chromophores, ε_0 the permittivity of vacuum and r_{AB} the distance between the interacting chromophores (center-to-center distance). α and θ are the rotational and translational offset angles, respectively, which result from the relative mutual orientation of the transition dipole moments of interacting molecules. According to this equation, the excitonic coupling strength maximizes for perfect collinear dimer stacks ($\alpha = 0^\circ$; $\theta = 90^\circ$) because only in this case the distance r_{AB} can be as small as ~3.5 Å. The most collinear arrangement is therefore given for dimers of dye **1 a** with an ε-value of 1180 cm^{-1} (Table 1). Very close to this value and, indeed, within the experimental error are the values for bis(merocyanine) dyes **1 i**–**k** with C7–C12 alkyl spacers (Table 2). For all other bis(merocyanine) dyes the less hypsochromically shifted aggregate band suggests a more twisted chromophore arrangement in the foldamers.

A quantification of the rotational displacement angle α between the two merocyanine chromophores in the foldamers may be accomplished under the assumptions that i) the translational displacement angle θ is equal to 90° for all foldamers as well as for the intermolecular dimer aggregates of reference dyes **1 a**,**b** (i.e., perfect co-facial stacking), ii) the transition dipole moment μ_{ag} of the involved chromophores and the distance r_{AB} between those are identical for all investigated dyes (i.e., close π–π-stacking at van-der-Waals distance), and iii) for dimer aggregates of the reference dyes **1 a**,**b** the rotational displacement angle α is equal to 0° (supported by the crystal structure[25] for **1 a**). Based on these assumptions, the quotient in Equation (10) is a constant and the term 3 $\cos^2\theta$ is equal to zero. Thus, the quantity of the excitonic splitting energy ε only depends on the cosinus of the angle α with $\varepsilon = 1180\ cm^{-1} \times \cos\alpha$. According to this simple analysis, the rotational displacements within the given foldamers are in the range from 14° (**1 i**–**k**) to 52° (**1 e**) that are quite reasonable values if we consider the significant number of simplifications made for this analysis. Obviously, the obtained results corroborate the view that the higher flexibility imparted by increasing spacer chain length should lead to dimer stacks with a more collinear arrangement of the transition dipole moments.

Conclusion

This work apparently constitutes the first investigation on the effect of various spacer units on the thermodynamics of folding for bichromophoric π-systems. By tethering two highly dipolar merocyanine chromophores with various spacers and performing concentration-dependent UV/Vis studies, we could distinguish between preferential *inter*molecular self-assembly into a quadruple dye stack (only one example) and the more general folding into *intra*molecular π-stacks (all other dyes). Our studies reveal that the final aggregate structure is essentially determined by the nature of the spacer. Thus, a rigid spacer that preorganizes the chromophores with an interplanar distance of roughly 7 Å results in the formation of a centrosymmetric bimolecular complex. This dye assembly comprises a π-stacked arrangement of four chromophores, excels with high binding strength ($>10^5\,M^{-1}$) in nonpolar dioxane and spectroscopically displays a more than 50 nm blue-shifted absorption maximum compared to that of the respective monomeric species. In contrast, the utilization of flexible linkers leads inevitably to the formation of intramolecular pleated structures, which are in a chemical equilibrium with disordered, unfolded species. Based on a solvent-dependent analysis of the free energy changes between these conformational states, we found that the folding tendency for different alkyl chain lengths shows a biphasic behavior, that is, a steep increase of the folding tendency from C4 to C7 and a subsequent less pronounced decrease for longer alkyl chains. Because the optical and electronic properties of such bichromophoric aggregate systems are strongly dependent on the respective aggregate geometry, our studies might pave the way towards tailored organic solid-state materials. Folding-driven modulation of optical and electronic properties of simply tethered bichromophores appears to be a quite attractive research avenue.

Experimental Section

For materials and methods and for the synthesis of precursor amides **3g**,**i**–**k** and hydroxypyridones **4c**,**e**–**k** see the Supporting Information.

Synthesis of target compounds 1c,e–k

***N,N′*-(*para*-Phenylenedimethylene)-bis(5-dibutylamino-thiophen-2-yl-methylene-4-methyl-2,6-dioxo-1,2,5,6-tetrahydropyridine-3-carbonitrile) (1c)**: A mixture of bis(pyridone) **4c** (200 mg, 497 μmol) and 5-(dibutylamino)thiophene-2-carbaldehyde (262 mg, 1.09 mmol) in Ac_2O (2 mL) was stirred at 90 °C for 120 min. The reaction mixture was treated with *i*PrOH and *n*-hexane, filtered and washed successively with *n*-hexane, Et_2O and toluene to give the crude product (336 mg, 80%) in a purity of ~80% (corresponding to a yield of ~64% of **1c**). Owing to the very poor solubility of **1c** only a small amount of the crude product was purified by column chromatography (silica gel, $CHCl_3$/MeOH 100:5 v/v) and subsequent precipitation from CH_2Cl_2/*n*-hexane for the characterization and UV/Vis spectroscopy. M.p. 305–306 °C; ^{1}H NMR (400 MHz, [D$_6$]DMSO): $\delta=8.02$ (d, $J=5.2$ Hz, 2H), 7.87 (s, 2H), 7.16 (s, 4H), 6.85 (d, $J=5.3$ Hz, 2H), 4.99 (s, 4H), 3.60–3.53 (m, 8H), 2.46 (s, 6H), 1.68–1.57 (m, 8H), 1.37–1.27 (m, 8H), 0.91 (t, $J=7.4$ Hz, 12H); ^{13}C NMR (151 MHz, [D$_6$]DMSO): $\delta=176.4$, 162.2, 161.3, 158.4, 153.8, 141.6, 136.2, 127.2, 124.4, 117.2, 112.7, 110.8, 105.2, 91.3, 53.1, 41.5, 28.5, 19.0, 13.1; UV/Vis (THF): λ_{max} (ε) = 536 nm ($251\,000\,M^{-1}cm^{-1}$); HRMS (ESI, acetonitrile/chloroform, pos. mode): *m/z* calcd for $C_{48}H_{56}N_6O_4S_2$: 844.3799, found: 844.3799 $[M]^+$; elemental analysis calcd (%) for $C_{48}H_{56}N_6O_4S_2$: C 68.22, H 6.68, N 9.94, S 7.59; found: C 68.20, H 6.76, N 9.87, S 7.36.

General procedure for the synthesis of bis(merocyanine) dyes 1e–k

A mixture of the respective pyridone acceptor **4e**–**k** and 2.2 equivalents of 5-dibutylaminothiophene-2-carbaldehyde in 2–6 mL Ac_2O was stirred at 90 °C for 60 min. After cooling to room temperature, the mixture was treated with EtOH/MeOH and the solvent was removed under reduced pressure. The crude products were purified by column chromatography (silica gel) and subsequent precipitation from CH_2Cl_2/*n*-hexane.

***N,N′*-Tetramethylene-bis(5-dibutylamino-thiophen-2-yl-methylene-4-methyl-2,6-dioxo-1,2,5,6-tetrahydropyridine-3-carbonitrile) (1e)**: Compound **1e** was synthesized according to the above general procedure using bis(pyridone) **4e** (150 mg, 423 μmol) and 5-dibutylaminothiophene-2-carbaldehyde (225 mg, 931 μmol) yielding a red solid (315 mg, 93%). Column chromatography was performed using dichloromethane/methanol (100:2) as eluent. M.p. 269–270 °C; ^{1}H NMR (400 MHz, CD_2Cl_2): $\delta=7.58$ (m, 4H), 6.41 (d, $J=5.2$ Hz, 2H), 3.97 (t, $J=5.4$ Hz, 4H), 3.55 (t, $J=7.7$ Hz, 8H), 2.46 (s, 6H), 1.78–1.68 (m, 8H), 1.65 (t, $J=5.4$ Hz, 4H), 1.47–1.37 (m, 8H), 0.99 (t, $J=7.3$ Hz, 12H); ^{13}C NMR (101 MHz, $CDCl_3$): $\delta=175.8$, 163.4, 162.4, 157.9, 151.9, 142.1, 124.5, 117.4, 110.3, 107.5, 95.3, 39.7, 29.8, 29.5, 25.5, 20.2, 18.9, 13.9; UV/Vis (CH_2Cl_2): λ_{max} (ε) = 540 nm ($264\,000\,M^{-1}cm^{-1}$); HRMS (ESI, acetonitrile/chloroform, pos. mode): *m/z* calcd for $C_{44}H_{56}N_6O_4S_2$ 796.3799, found: 796.3802 $[M]^+$.

***N,N′*-Pentamethylene-bis(5-dibutylamino-thiophen-2-yl-methylene-4-methyl-2,6-dioxo-1,2,5,6-tetrahydropyridine-3-carbonitrile) (1f)**: Compound **1f** was synthesized according to the above general procedure using bis(pyridone) **4f** (200 mg, 543 μmol) and 5-dibutylaminothiophene-2-carbaldehyde (273 mg, 1.14 mmol) yielding a red solid (280 mg, 64%). Column chromatography was performed using dichloromethane/methanol (100:2) as eluent. M.p. 171–172 °C; ^{1}H NMR (400 MHz, CD_2Cl_2): $\delta=7.56$ (d, $J=5.2$ Hz, 2H), 7.54 (s, 2H), 6.40 (d, $J=5.2$ Hz, 2H), 3.94 (t, $J=7.4$ Hz, 4H), 3.53 (t, $J=7.6$ Hz, 8H), 2.44 (s, 6H), 1.81–1.61 (m, 12H), 1.47–1.36 (m, 10H), 0.98 (t, $J=7.4$ Hz, 12H); ^{13}C NMR (101 MHz, CD_2Cl_2): $\delta=176.3$, 163.6, 162.5, 158.3, 152.5, 142.1, 124.7, 117.8, 111.2, 107.3, 94.7, 54.2 (overlapped with solvent signal), 39.9, 29.6, 28.1, 25.1, 20.4, 18.9, 13.9; UV/Vis (CH_2Cl_2): λ_{max} (ε) = 539 nm ($277\,000\,M^{-1}cm^{-1}$); HRMS (ESI, acetonitrile/chloroform, pos. mode): *m/z* calcd for $C_{45}H_{58}N_6O_4S_2$: 810.3956, found: 810.3963 $[M]^+$; elemental analysis calcd (%) for $C_{45}H_{58}N_6O_4S_2$: C 66.63, H 7.21, N 10.36, S 7.91; found: C 66.39, H 7.34, N 10.29, S 7.87.

***N,N′*-[2,2′-Oxybis(dimethylene)]-bis(5-dibutylamino-thiophen-2-yl-methylene-4-methyl-2,6-dioxo-1,2,5,6-tetrahydropyridine-3-carbonitrile) (1g)**: Compound **1g** was synthesized according to the above general procedure using bis(pyridone) **4g** (300 mg, 810 μmol) and 5-dibutylaminothiophene-2-carbaldehyde (427 mg, 1.78 mmol) yielding a red solid (532 mg, 81%). Column chromatography was performed using chloroform/methanol (100:7) as eluent. M.p. 215–216 °C; ^{1}H NMR (400 MHz, $CDCl_3$): $\delta=7.50$ (d, $J=5.1$ Hz, 2H), 7.47 (s, 2H), 6.35 (d, $J=5.1$ Hz, 2H), 4.21 (t, $J=6.2$ Hz, 4H), 3.76 (t, $J=6.3$ Hz, 4H), 3.54 (t, $J=7.8$ Hz, 8H), 2.41 (s, 6H), 1.78–1.68 (m, 8H), 1.47–1.37 (m, 8H), 0.99 (t, $J=7.4$ Hz, 12H); ^{13}C NMR (101 MHz, $CDCl_3$): $\delta=176.0$, 163.5, 162.3, 158.1, 152.1, 141.9, 124.7, 117.4, 110.7, 107.2, 94.8, 67.6, 53.9, 38.9, 29.5, 20.2, 18.8, 13.9; UV/Vis (CH_2Cl_2): λ_{max} (ε) = 538 nm ($248\,000\,M^{-1}cm^{-1}$); HRMS (ESI, acetonitrile/chloroform, pos. mode): *m/z* calcd for $C_{44}H_{56}N_6O_5S_2$:

812.3748, found: 812.3750 $[M]^+$; elemental analysis calcd (%) for $C_{44}H_{56}N_6O_5S_2$: C 65.00, H 6.94, N 10.34, S 7.89; found: C 64.74, H 7.30, N 10.04, S 7.60.

***N,N′*-Hexamethylene-bis(5-dibutylamino-thiophen-2-yl-methylene-4-methyl-2,6-dioxo-1,2,5,6-tetrahydropyridine-3-carbonitrile) (1 h)**: Compound **1 h** was synthesized according to the above general procedure using bis(pyridone) **4 h** (100 mg, 262 μmol) and 5-dibutylaminothiophene-2-carbaldehyde (138 mg, 575 μmol) yielding a red solid (182 mg, 84%). Column chromatography was performed using dichloromethane/methanol (100:2) as eluent. M.p. 269–270 °C; ^{1}H NMR (400 MHz, CD_2Cl_2): $\delta = 7.58$ (m, 4H), 6.40 (d, $J = 5.1$ Hz, 2H), 3.93 (t, $J = 7.5$ Hz, 4H), 3.53 (t, $J = 7.7$ Hz, 8H), 2.46 (s, 6H), 1.77–1.68 (m, 8H), 1.66–1.56 (m, 4H), 1.47–1.36 (m, 12H), 0.99 (t, $J = 7.4$ Hz, 12H); ^{13}C NMR (101 MHz, CD_2Cl_2): $\delta = 176.2$, 163.7, 162.5, 158.3, 152.4, 142.3, 124.6, 117.8, 111.0, 107.4, 95.1, 53.6 (overlapped with solvent signal), 40.0, 29.6, 28.3, 27.3, 20.5, 18.9, 13.9; UV/Vis (CH_2Cl_2): λ_{max} (ε) = 539 nm (279000 $M^{-1}cm^{-1}$); HRMS (ESI, acetonitrile/chloroform, pos. mode): *m/z* calcd for $C_{46}H_{60}N_6O_4S_2$: 824.4112, found: 824.4118 $[M]^+$; elemental analysis calcd (%) for $C_{46}H_{60}N_6O_4S_2$: C 66.96, H 7.33, N 10.19, S 7.77; found: C 67.28, H 7.40, N 10.27, S 7.77.

***N,N′*-Heptamethylene-bis(5-dibutylamino-thiophen-2-yl-methylene-4-methyl-2,6-dioxo-1,2,5,6-tetrahydropyridine-3-carbonitrile) (1 i)**: Compound **1 i** was synthesized according to the above general procedure using bis(pyridone) **4 i** (150 mg, 378 μmol) and 5-dibutylaminothiophene-2-carbaldehyde (200 mg, 832 μmol) yielding a red solid (205 mg, 65%). Column chromatography was performed using dichloromethane/methanol (100:2) as eluent. M.p. 149–150 °C; ^{1}H NMR (400 MHz, CD_2Cl_2): $\delta = 7.58$ (m, 4H), 6.40 (d, $J = 5.2$ Hz, 2H), 3.92 (t, $J = 7.5$ Hz, 4H), 3.54 (t, $J = 7.7$ Hz, 8H), 2.46 (s, 6H), 1.77–1.68 (m, 8H), 1.65–1.56 (m, 4H), 1.47–1.33 (m, 14H), 0.99 (t, $J = 7.3$ Hz, 12H); ^{13}C NMR (101 MHz, CD_2Cl_2): $\delta = 176.2$, 163.7, 162.5, 158.2, 152.4, 142.2, 124.6, 117.8, 111.0, 107.5, 95.0, 53.8 (overlapped with solvent signal), 40.0, 29.6, 29.5, 28.2, 27.4, 20.5, 18.9, 13.9; UV/Vis (CH_2Cl_2): λ_{max} (ε) = 539 nm (272000 $M^{-1}cm^{-1}$); HRMS (ESI, acetonitrile/chloroform, pos. mode): *m/z* calcd for $C_{47}H_{62}N_6O_4S_2$: 838.4269, found: 838.4266 $[M]^+$; elemental analysis calcd (%) for $C_{47}H_{62}N_6O_4S_2$: C 67.27, H 7.45, N 10.01, S 7.64; found: C 66.98, H 7.56, N 9.93, S 7.40.

***N,N′*-Octamethylene-bis(5-dibutylamino-thiophen-2-yl-methylene-4-methyl-2,6-dioxo-1,2,5,6-tetrahydropyridine-3-carbonitrile) (1 j)**: Compound **1 j** was synthesized according to the above general procedure using bis(pyridone) **4 j** (100 mg, 244 μmol) and 5-(dibutylamino)-thiophene-2-carbaldehyde (130 mg, 536 μmol) yielding a red solid (157 mg, 76%). Column chromatography was performed using dichloromethane/methanol (100:2) as eluent. M.p. 224–225 °C; ^{1}H NMR (400 MHz, CD_2Cl_2): $\delta = 7.58$ (m, 4H), 6.40 (d, $J = 5.2$ Hz, 2H), 3.92 (t, $J = 7.5$ Hz, 4H), 3.54 (t, $J = 7.7$ Hz, 8H), 2.47 (s, 6H), 1.78–1.68 (m, 8H), 1.64–1.54 (m, 4H), 1.47–1.33 (m, 16H), 0.99 (t, $J = 7.3$ Hz, 12H); ^{13}C NMR (101 MHz, CD_2Cl_2): $\delta = 176.1$, 163.7, 162.5, 158.2, 152.4, 142.3, 124.6, 117.8, 111.0, 107.5, 95.1, 53.8 (overlapped with solvent signal), 40.0, 29.8, 29.6, 28.2, 27.5, 20.5, 18.9, 13.9; UV/Vis (CH_2Cl_2): λ_{max} (ε) = 539 nm (277000 $M^{-1}cm^{-1}$); HRMS (ESI, acetonitrile/chloroform, pos. mode): *m/z* calcd for $C_{48}H_{64}N_6O_4S_2$: 852.4425, found: 852.4428 $[M]^+$; elemental analysis calcd (%) for $C_{48}H_{64}N_6O_4S_2$: C 67.57, H 7.56, N 9.85, S 7.52; found: C 67.51, H 7.59, N 9.78, S 7.30.

***N,N′*-Dodecamethylene-bis(5-dibutylamino-thiophen-2-yl-methylene-4-methyl-2,6-dioxo-1,2,5,6-tetrahydropyridine-3-carbonitrile) (1 k)**: Compound **1 k** was synthesized according to the above general procedure using bis(pyridone) **4 k** (150 mg, 322 μmol) and 5-(dibutylamino)thiophene-2-carbaldehyde (170 mg, 707 μmol) yielding a red solid (175 mg, 60%). Column chromatography was performed using dichloromethane/methanol (100:2) as eluent. M.p. 264–265 °C; ^{1}H NMR (400 MHz, CD_2Cl_2): $\delta = 7.61$ (m, 4H), 6.41 (d, $J = 5.2$ Hz, 2H), 3.92 (t, $J = 7.5$ Hz, 4H), 3.54 (t, $J = 7.7$ Hz, 8H), 2.48 (s, 6H), 1.78–1.68 (m, 8H), 1.64–1.54 (m, 4H), 1.47–1.33 (m, 16H), 0.99 (t, $J = 7.3$ Hz, 12H); ^{13}C NMR (101 MHz, CD_2Cl_2): $\delta = 176.1$, 163.7, 162.5, 158.3, 152.5, 142.4, 124.6, 117.8, 111.0, 107.5, 95.3, 53.8 (overlapped with solvent signal), 40.0, 30.0, 29.8, 29.6, 28.3, 27.5, 20.5, 19.0, 13.9; UV/Vis (CH_2Cl_2): λ_{max} (ε) = 540 nm (289000 $L mol^{-1} cm^{-1}$); HRMS (ESI, acetonitrile/chloroform, pos. mode): *m/z* calcd for $C_{52}H_{72}N_6O_4S_2$: 908.5051, found: 908.5048 $[M]^+$; elemental analysis calcd (%) for $C_{52}H_{72}N_6O_4S_2$: C 68.69, H 7.98, N 9.24, S 7.05; found: C 68.79, H 8.14, N 9.27, S 6.84.

Keywords: dipolar interaction · dyes/pigments · excitonic coupling · foldamers · self-assembly

[1] F. C. Spano, *Acc. Chem. Res.* **2010**, *43*, 429 – 439.
[2] V. Coropceanu, J. Cornil, D. A. da Silva, Y. Olivier, R. Silbey, J. L. Bredas, *Chem. Rev.* **2007**, *107*, 926 – 952.
[3] a) R. Bhosale, J. Misek, N. Sakai, S. Matile, *Chem. Soc. Rev.* **2010**, *39*, 138 – 149; b) D. M. Bassani, L. Jonusauskaite, A. Lavie-Cambot, N. D. McClenaghan, J. L. Pozzo, D. Ray, G. Vives, *Coord. Chem. Rev.* **2010**, *254*, 2429 – 2445; c) M. R. Wasielewski, *Acc. Chem. Res.* **2009**, *42*, 1910 – 1921; d) F. Würthner, T. E. Kaiser, C. R. Saha-Möller, *Angew. Chem. Int. Ed.* **2011**, *50*, 3376 – 3410; *Angew. Chem.* **2011**, *123*, 3436 – 3473.
[4] a) T. Aida, E. W. Meijer, S. I. Stupp, *Science* **2012**, *335*, 813 – 817; b) S. Babu, S. Sukumara, V. K. Praveen, A. Ajayaghosh, *Chem. Rev.* **2014**, *114*, 1973 – 2129; c) A. P. H. J. Schenning, D. Gonzalez-Rodriguez, *Chem. Mater.* **2011**, *23*, 310 – 325; d) S. Yagai, *Bull. Chem. Soc. Jpn.* **2015**, *88*, 28 – 58.
[5] a) L. Lu, R. J. Lachicotte, T. L. Penner, J. Perlstein, D. G. Whitten, *J. Am. Chem. Soc.* **1999**, *121*, 8146 – 8156; b) S. Zeena, K. G. Thomas, *J. Am. Chem. Soc.* **2001**, *123*, 7859 – 7865; c) E. Arunkumar, A. Ajayaghosh, J. Daub, *J. Am. Chem. Soc.* **2005**, *127*, 3156 – 3164.
[6] a) D.-W. Zhang, X. Zhao, J.-L. Hou, Z.-T. Li, *Chem. Rev.* **2012**, *112*, 5271 – 5316; b) G. Gilles, I. Huc, *Chem. Commun.* **2011**, *47*, 5933 – 5941; c) S. Ishu, A. D. Hamilton, *Chem. Soc. Rev.* **2009**, *38*, 1726 – 1743; d) M. S. Cubberley, B. L. S. Iverson, *Curr. Opin. Chem. Biol.* **2001**, *5*, 650 – 653; e) H. Gellman, *Acc. Chem. Res.* **1998**, *31*, 173 – 180; f) S. Hecht, I. Huc, *Foldamers: Structure, Properties and Applications*, Wiley-VCH, Weinheim, **2007**.
[7] J. M. Berg, J. L. Tymoczko, L. Stryer, *Biochemistry*; W. H. Freeman, San Francisco, **2010**.
[8] a) J. D. Tovar, *Acc. Chem. Res.* **2013**, *46*, 1527 – 1537; b) L. C. Palmer, S. I. Stupp, *Acc. Chem. Res.* **2008**, *41*, 1674 – 1684.
[9] a) U. Lewandowska, W. Zajaczkowski, L. Chen, F. Bouillière, D. Wang, K. Koynov, W. Pisula, K. Müllen, H. Wennemers, *Angew. Chem. Int. Ed.* **2014**, *53*, 12537 – 12541; *Angew. Chem.* **2014**, *126*, 12745 – 12749; b) W. M. Park, J. A. Champion, *J. Am. Chem. Soc.* **2014**, *136*, 17906 – 17909; c) J. P. Schneider, D. J. Pochan, B. Ozbas, K. Rajagopal, L. Pakstis, J. Kretsinger, *J. Am. Chem. Soc.* **2002**, *124*, 15030 – 15037.
[10] W. S. Horne, S. H. Gellman, *Acc. Chem. Res.* **2008**, *41*, 1399 – 1408.
[11] a) S. C. Zimmerman, *Topics Curr. Chem.* **1993**, *165*, 71 – 102; b) F.-G. Klärner, B. Kahlert, *Acc. Chem. Res.* **2003**, *36*, 919 – 932.
[12] a) A. Das, S. Ghosh, *Chem. Commun.* **2014**, *50*, 11657 – 11660; b) S. Ghosh, S. Ramakrishnan, *Angew. Chem. Int. Ed.* **2004**, *43*, 3264 – 3268; *Angew. Chem.* **2004**, *116*, 3326 – 3330; c) A. D. Q. Li, *Chem. Eur. J.* **2003**, *9*, 4594 – 4601.
[13] F. Würthner, S. Yao, T. Debaerdemaeker, R. Wortmann, *J. Am. Chem. Soc.* **2002**, *124*, 9431 – 9447.
[14] a) Z. Chen, A. Lohr, C. R. Saha-Möller, F. Würthner, *Chem. Soc. Rev.* **2009**, *38*, 564 – 584; b) C. A. Hunter, *Chem. Soc. Rev.* **1994**, *23*, 101 – 109.
[15] A. Zitzler-Kunkel, M. R. Lenze, K. Meerholz, F. Würthner, *Chem. Sci.* **2013**, *4*, 2071 – 2075.
[16] F. Würthner, S. Yao, J. Schilling, R. Wortmann, M. Redi-Abshiro, E. Mecher, F. Gallego-Gomez, K. Meerholz, *J. Am. Chem. Soc.* **2001**, *123*, 2810 – 2824.
[17] A. Lohr, F. Würthner, *Isr. J. Chem.* **2011**, *51*, 1052 – 1066.
[18] M. Kasha, *Radiat. Res.* **1963**, *20*, 55 – 70.

[19] M. Kasha, H. R. Rawls, M. A. El-Bayoumi, *Pure Appl. Chem.* **1965**, *11*, 371 – 392.
[20] U. Rösch, S. Yao, R. Wortmann, F. Würthner, *Angew. Chem. Int. Ed.* **2006**, *45*, 7026 – 7030; *Angew. Chem.* **2006**, *118*, 7184 – 7188.
[21] F. Würthner, S. Yao, *Angew. Chem. Int. Ed.* **2000**, *39*, 1978 – 1981; *Angew. Chem.* **2000**, *112*, 2054 – 2057.
[22] F. Würthner, S. Yao, U. Beginn, *Angew. Chem. Int. Ed.* **2003**, *42*, 3247 – 3250; *Angew. Chem.* **2003**, *115*, 3368 – 3371.
[23] A. Lohr, T. Greß, M. Deppisch, M. Knoll, F. Würthner, *Synthesis* **2007**, *19*, 3073 – 3082.
[24] a) B. Odell, M. V. Reddington, A. M. Z. Slawin, N. Spencer, J. F. Stoddart, D. J. Williams, *Angew. Chem. Int. Ed. Engl.* **1988**, *27*, 1547 – 1550; *Angew. Chem.* **1988**, *100*, 1605 – 1608; b) E. J. Dale, N. A. Vermeulen, A. A. Thomas, J. C. Barnes, M. Juricek, A. K. Blackburn, N. L. Strutt, A. A. Sarjeant, C. L. Stern, S. E. Denmark, J. F. Stoddart, *J. Am. Chem. Soc.* **2014**, *136*, 10669 – 10682.
[25] A. Zitzler-Kunkel, M. R. Lenze, N. M. Kronenberg, A.-M. Krause, M. Stolte, K. Meerholz, F. Würthner, *Chem. Mater.* **2014**, *26*, 4856 – 4866.
[26] T. F. A. De Greef, M. M. J. Smulders, M. Wolffs, A. P. H. J. Schenning, R. P. Sijbesma, E. W. Meijer, *Chem. Rev.* **2009**, *109*, 5687 – 5754.
[27] R. B. Martin, *Chem. Rev.* **1996**, *96*, 3043 – 3064.
[28] G. Fernández, M. Stolte, V. Stepanenko, F. Würthner, *Chem. Eur. J.* **2013**, *19*, 206 – 217.
[29] C. A. Hunter, H. L. Anderson, *Angew. Chem. Int. Ed.* **2009**, *48*, 7488 – 7499; *Angew. Chem.* **2009**, *121*, 7624 – 7636.
[30] C. R. Ray, J. S. Moore, *Adv. Polym. Sci.* **2005**, *177*, 91 – 149.
[31] C. N. Pace, B. A. Shirley, J. A. Thompson, *Protein Structure: A Practical Approach*, IRL Press, New York, **1989**.
[32] G. Whitesides, J. Mathias, C. Seto, *Science* **1991**, *254*, 1312 – 1319.
[33] F. May, V. Marcon, M. R. Hansen, F. Grozema, D. Andrienko, *J. Mater. Chem.* **2011**, *21*, 9538 – 9545.

Received: June 23, 2015
Published online on September 8, 2015